Volumetric Texture Analysis based on Three-Dimensional Gaussian Markov Random Fields for COPD Detection

Yasseen Almakady[1], Sasan Mahmoodi[1], Joy Conway [2,3], Michael Bennett [3]

1 Faculty of Physical Sciences and Engineering , University of Southampton, Highfield Campus, Southampton, SO17 1BJ, United Kingdom.
2 Faculty of Health Sciences, University of Southampton, Highfield Campus, Southampton, SO17 1BJ, United Kingdom.
3 Southampton NIHR Respiratory and Critical Care Biomedical Re-search Centre, University Hospital Southampton NHS Foundation Trust, Southampton SO16 6YD, United Kingdom
{yham1n15,sm3y07,jhc,michael.bennett}@soton.ac.uk

Abstract. This paper proposes a 3D GMRF-based descriptor for volumetric texture image classification. In our proposed method, the estimated parameters of the GMRF model in volumetric texture images are employed as texture features in addition to the mean of a processed image region. The descriptor of the volumetric texture is then constructed by computing the histograms of each feature element to characterize the local texture. The evaluation of this descriptor achieves a high classification accuracy on a 3D synthetic texture database. Our method is then applied on a clinical dataset to exploit its discriminatory power, achieving a high classification accuracy in COPD detection. To demonstrate the performance of the descriptor, a comparison is carried out against a 2D GMRF-based method using the same dataset, variables, and settings. The descriptor outperforms the 2D GMRF-based method by a significant margin.

Keywords: COPD, 3D GMRF, Volumetric Texture.

1 Introduction

In recent years, chronic obstructive pulmonary disease (COPD), which refers to a group of progressive lung diseases, has become a serious disease emerging gradually worldwide. According to [1], by 2020 it is projected to rank third in significant causes of death worldwide. Despite important efforts that have been made over the past two decades, some significant issues have not been addressed including the mechanisms of disease and early diagnosis [2]. Therefore, additional research methods are necessary to develop new solutions and treatments of this disease. Medical image analysis using computer vision techniques can potentially provide robust solutions that support diagnosis.

COPD is defined as "a common, preventable, and treatable disease characterized by persistent respiratory symptoms and airflow limitation that is due to airway and/or alveolar abnormalities" [3]. There are many signs and symptoms that can be identified in patients with COPD. These symptoms include a chronic cough, which is often the first symptom. In addition to this, shortness of breath, wheezing, and sputum production are also critical symptoms of this disease [3]. Although these symptoms are key to diagnosis of this disease, automated analysis of COPD has received considerable research interest [27,28,29].

The common clinical diagnostic tool for COPD is Spirometry which concerns performing a Pulmonary Function test (PFT) to measure lung condition [3,4]. Computed Tomography (CT) is another growing diagnostic tool that is capable of diagnosing COPD, providing more information about the type of disease, severity [4] and distribution throughout the lung. This is one of the key advantages of imaging based approaches – that they allow us to determine where in the lung the disease is (COPD tends to be very heterogeneous, with some parts of the lung remaining completely healthy, whilst other parts are affected by disease. Spirometry cannot give this kind of information.

Many methods have been proposed to quantify emphysema, a common disease classified under COPD, focused on density histogram as features. The emphysema index or density mask was among early methods, introduced in [5], mainly aimed at measuring attenuation values below a certain threshold using consequent information as features. Another important quantification method for the diagnosis of this disease was proposed based on texture features. The popular Local Binary Pattern (LBP) method that was originally proposed in [6] was used to extract the feature values from different regions of interest (ROIs). The features histogram is therefore computed and used to classify ROIs [4]. Recently, features extracted by co-occurrence matrices to capture spatial dependence of gray-level intensities and Gaussian derivative methods to capture structural features was proposed to automatically detect emphysema without local annotation [7]. Moreover, a method of combining multiple features has been reported in [8] whereas texture and intensity features are integrated to perform quantification of emphysema in high-resolution computed tomography (HRCT), claiming that adopting additional features such as the texture improves the performance of the proposed method.

1.1 Texture-based Features

Texture is an important feature of many types of images such as medical, natural, and industrial images. Feature extraction and analysis from textures are important topics in image processing and computer vision particularly in medical image analysis. Recently, texture analysis problems have been widely studied delivering various solutions. These problems can be generally classified into four main categories: image classification, image segmentation, image synthesis, and texture-based shape extraction [9].

In recent years, a wide variety of methods have been for the analysis of texture, one of which is a model-based method which uses a generative image to represent the image [10] such as an autoregressive module [11]. Markov random fields (MRF) and its subclass Gaussian Markov random fields (GMRF) are examples of model-based methods.

However, recent advances in medical imaging, which offer three-dimensional (3D) imaging, have created issues related to feature extraction of volumetric images because applying 2D methods on 3D images result in the loss of important information. This has led to the extension of many 2D texture methods to 3D extended methods such as work in [12,13,14], while some efficient methods still need to be extended in order to exploit their capability of handling 3D texture. The excellent performance of the methods based GMRF presented in [18,22] inspire us to extend them to deal with textures in 3D volumetric images to the best of our knowledge; these methods have not yet been extended to handle the case of 3D volumetric image data.

1.2 Volumetric Texture

Texture can be defined as a spatial arrangement of the gray values of neighboring pixels [15]. This spatial arrangement of gray values on a surface known as 2D texture can be easily observed by human perception. In contrast, 3D texture images represented by more than two dimensions are impossible to be fully visualized by human perception [16]. Volumetric texture or solid texture is an example of 3D texture, which is indexed by three coordinates [17]. This paper considers the 'volumetric texture' represented by $(x, y, z) \in \mathbb{R}^3$ in a 3D coordinate system. This type of texture widely exists in the medical imaging fields representing the internal structure of human organs such as the brain and lungs. Figure 1 shows an HRCT image of a left lung displaying the interior structure of the lung.

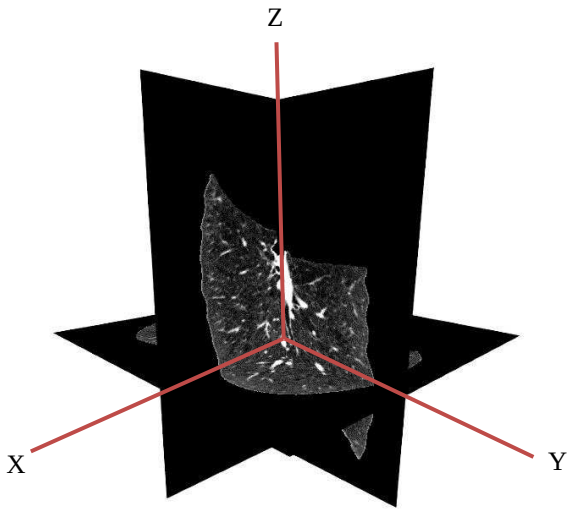

Fig. 1. The interior structure of a left lung in an HRCT image.

This paper aims to characterize textures in volumetric images based on the 3D GMRF model to develop a computer-aided utility for automatic COPD diagnosis by extracting texture-based features from HRCT volumetric images.

The remainder of this paper is organized as follows: Section 2 introduces our method and some related issues in detail. In section 3, the results of method evaluation are presented. Section 4 compares the application of the method in medical images to another method and section 5 concludes the paper and outlines future work.

2 Three-dimensional Gaussian Markov Random Fields Model (3D GMRF)

MRFs have been a popular model-based method for texture analysis due to their ability to characterize local spatial information in an image [30]. This method obeys the Markovian property in which each pixel depends directly on the neighboring pixels. GMRF, a sub-class of MRF, is among the most popular model-based method for texture classification [18].

Let $\Omega_v = \{v = (i,j,k) \mid 1 \leq i \leq H, 1 \leq j \leq W, 1 \leq k \leq D\}$ denote the set of voxels indexed by (i,j,k) on a $H \times W \times D$ 3D lattice corresponding to voxels in three-dimensional image volume. The local conditional probability density function of the intensity value g_v at location v is defined by:

$$p(g_v|y_r, r \in V) = \frac{1}{\sqrt{2\pi\sigma^2}} \exp\left\{ -\frac{1}{2\sigma^2}\left(g_v - \lambda - \sum_{r \in V} \alpha_r (y_r - \lambda) \right)^2 \right\} \quad (1)$$

where V are the neighbors of the voxel at location v, α_r are the interaction parameters that measure the influence on a voxel by neighbors' intensity values y_r located at a relative position r [18,19]. The neighborhood scheme adopted here is sampled voxels over a sphere surface with radius R, so that $V \in \{\theta, \phi \mid 0 \leq \theta \leq \pi,\ 0 \leq \phi \leq 2\pi\}$ and $|V|$ is equivalent to the number of voxels. Figure 2 presents the sampled voxels over a sphere equivalent to the neighbors y_r, where the center of the sphere corresponds to g_v, which is used to collect observations.

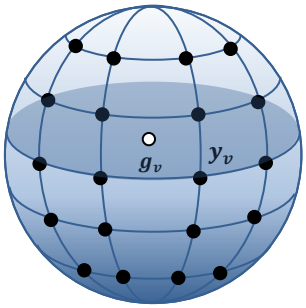

Fig. 2. Graphical representation of voxels y_v sampled over a sphere where g_v is the central voxel.

2.1 Parameter Estimation

The model parameters in equation (1) can be estimated using two common methods; the maximum likelihood estimation (MLE) and least squares estimation (LSE). Although both methods produce adequate results and lead to the same set of equations in terms of GMRF, MLE has many advantages over LSE [20]. Further from being fast and easy to implement, MLE provides an optimal estimation in large samples while it is also consistent in small samples. As a result, MLE is selected for the GMRF model parameters estimation.

MLE is found by taking the partial derivative of a log-likelihood function with respect to α, σ, λ and setting it to zero leads to the following simultaneous equations:

$$Z\,(1-\alpha_v)\lambda = \sum_{v\in\Omega_v}(g_v - \alpha_v y_v) \tag{2}$$

$$-\lambda\sum_{v\in\Omega_v} y_k + \sum_{v\in\Omega_v} y_k\alpha_v\,(y_v-\lambda) = \sum_{v\in\Omega_v} g_v\,y_k \quad ,k\ \in r \tag{3}$$

$$\sigma^2 = \sum_{v\in\Omega_v}(g_v - \lambda - \alpha_v(y_v-\lambda))^2 \tag{4}$$

where $Z = H\times W\times D$, $\alpha_v = row[a_r]$ and $y_v = col[y_r]$ for $r\in V$ .These model parameters α, σ^2 and λ are calculated by solving simultaneous equations (2–4) and therefore employed as features vector $f_v = [\alpha, \sigma^2, \lambda]$ for each voxel site v in the volume to characterize image texture and assumed to be constant over a particular voxel site.

2.2 Estimation Cube

In a 2D texture image, the GMRF model parameters estimation is carried out by sliding a $n\times n$ window over the texture image to collect sample observations. However, extracted features from small regions (blocks) is a preferred method when dealing with texture to characterize the local texture [21–23,31–33]. Therefore, instead of estimating parameters over the entire image, we follow the idea presented in [22] that propose a method in which parameter estimation is conducted in a small estimation window $w\ \times\ w$ with w equals to $2n-1$ where n is the neighborhood size. This is to ensure enough samples are provided to obtain a unique solution at the parameter estimation stage.

As a result, in volumetric texture, where there are three dimensions, the region becomes a cube leading to an estimation cube instead of an estimation window and the volume used to generate the observation inside the cube estimation is a sphere with R radius and $|V|$ sampled voxels. Figure 2 presents the sphere of the observation generator.

2.3 Descriptor Construction

The 3D GMRF texture feature consists of estimated parameters, including variance, for each voxel in the site Ω_v. The descriptor $GMRF_{P,R}^{3D}$ is therefore constructed by computing the distribution of each estimated parameter in the model to characterize the texture. In detail, a sphere with radius R and the number of sampled voxels equal to $|V|$ is slid inside the estimation cube with size w^3 to generate observation samples. At the same time, the estimation cube is also slid over the volume to achieve localization. Next, parameter estimations are carried out at each voxel producing a set of parameters for each voxel, leading to a feature vector obtained by:

$$f_v = \{\alpha, \sigma^2, \lambda\} \tag{5}$$

Distributions of each estimated parameter α, σ^2 and λ are therefore computed producing one histogram for each, then the descriptor is constructed by concatenating all histograms. The complete descriptor is given by:

$$GMRF_{P,R}^{3D} = \{H(\alpha_1), H(\alpha_2), H(\alpha_3), \ldots, H(\alpha_r), H(\sigma^2), H(\lambda)\} \tag{6}$$

where H is the histogram of each parameter, superscript ^{3D} indicates to 3D volumetric texture, while P, R refer respectively to the sampling rate of voxels placed on the sphere used for generating observations and its radius. Figure 3 shows an illustration of the proposed methods.

$GMRF_{P,R}^{3D}$ is employed as the descriptor for volumetric texture images and by setting P and R to different values, the descriptor can capture features at different spatial resolutions.

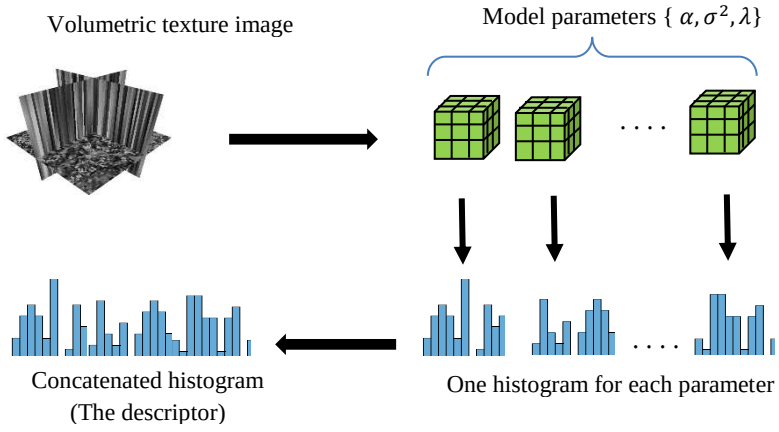

Fig. 3. An overview of the proposed method.

2.4 Implementation Issues

The first issue is to solve the simultaneous equations (2–4). These equations are non-linear with respect to λ. Such nonlinear equations are numerically more expensive to solve and may also suffer from instability; solving equation (2-4) imply dealing with nonlinear system. To avoid nonlinearity, we estimate the mean λ separately by calculating λ and subtracting it from the observation space Ω_v and then including it as a feature together with model parameters , the final solution leads to :

$$\alpha_v = \left(\sum_{v \in \Omega_v} y_v y_v^T \right)^{-1} \left(\sum_{v \in \Omega_v} y_v g_v \right) \tag{7}$$

$$\sigma_v^2 = \frac{1}{|\Omega_v|} \sum_{v \in \Omega_v} (g_v - \alpha_v y_v)^2 \tag{8}$$

The size of the $GMRF_{P,R}^{3D}$ descriptor depends on the number of voxel samples on the sphere and the histogram bins setting for each parameter. The size is given as follows:

$$\left| GMRF_{P,R}^{3D} \right| = (|V| + 2) * b \tag{9}$$

Where $|V|$ is the number of voxels, while b is the number of histogram bins and the additional values refer to the variance parameter σ^2 and the mean λ.

Another issue is encountered during the stage of parameter estimation, especially when inverting the parameters matrix causing a non-invertibility issue. The non-invertibility issue occurs when the observations matrix has no inverse and therefore becomes a singular matrix where no solution exists, leading to an inconsistent model. To overcome this issue, we must ensure that the observation matrix is non-singular and invertible. This can be achieved using various methods and one possible direct numerical solution is to use ridge regression by adding a regularization to the observation matrix in a way that will make it non-singular and invertible [24,25]. The interaction parameters α as a result are given by:

$$\alpha_v = \left(\sum_{v \in \Omega_v} y_v y_v^T + c^2 I \right)^{-1} \left(\sum_{v \in \Omega_v} y_v g_v \right) \tag{10}$$

where I is the identity matrix with a size equal to the size of the observation matrix and c is a constant number to control the strength of regularization. This is to be added

to the diagonal of the $y_v y_v^T$ observation matrix before the inversion operation to make the matrix non-singular.

The selection of the value c is not straightforward; we empirically choose the value that maximizes the accuracy of the classification.

3 Results and Discussion

In this section we aim to evaluate our descriptor through performing a classification on volumetric textures; we consider classification accuracies and the confusion matrix as classification measures for our descriptor.

3.1 Dataset

We evaluated our descriptor on a dataset for volumetric texture, or solid texture as referred by the creator in [26]. This dataset is constructed using a two-dimensional dataset such as Brodatz textures and fractal textures. One of the methods employed to generate this dataset interpolates two or more two-dimensional texture images to construct volumetric texture used in our evaluation. The dataset generated by the interpolation method contains 30 different classes composed of ten volumetric images, each corresponding to 64 two-dimensional texture images with a size of 64×64. We developed a simple program that easily constructs the volumetric texture at size 64^3. Figure 4 shows an example of volumetric texture from selected classes.

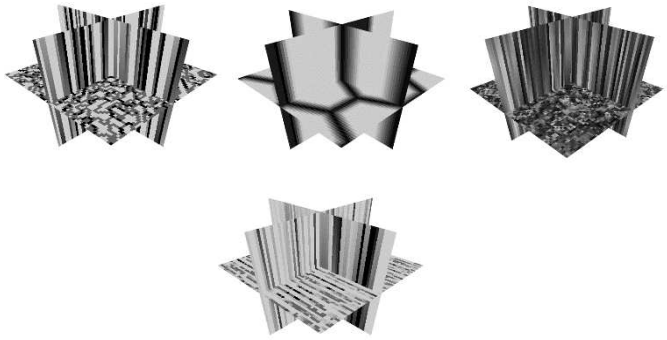

Fig. 4. Example of volumetric texture from a solid textures dataset [26] built using the interpolation method.

3.2 Evaluation Methods and Parameter Settings

First, it is important to set related variables to the desired values. Considering the size of the neighborhood, it is controlled by $2r + 1$, with spatial resolution $r = 1$. This radius covers a space of size 3^3 voxels. The number of voxels sampled over the sphere

depends on the number of equally-spaced points arranged on θ and ϕ , as we set $p = 16$, the total number of voxels is obtained by $|V| = p^2/2$. The size of the estimation cube is selected to be $w = 5$. Regarding the histogram, the number of bins is empirically selected to give the best result. The number of features, multiplied by the number of histogram bins, gives the size of the descriptor (see formula 9).

The descriptor is therefore constructed as described in section 2.3 and illustrated in Figure 3.

Classification is performed using k-nearest-neighbors kNN ($k = 1$) with the distance metric L1-norm. The accuracy of the classification is obtained by employing a leave-one-out scheme then the mean of accuracies over all classes is computed.

Table 1 shows classification accuracies for the descriptor obtained by performing $GMRF_{8,1}^{3D}$ and $GMRF_{16,1}^{3D}$ with a different number of sampling equivalent to $p = \{8,16\}$. The descriptor successfully classifies 98% of classes at a sampling rate of $p = 16$ while it produces an acceptable performance using only a sampling rate of $p = 8$, achieving an accuracy of 96%.

Table 1. Classification accuracies [%] for $GMRF_{P,R}^{3D}$ descriptor.

$GMRF_{P,R}^{3D}$	Number of Histogram bins						
	5	10	20	30	50	65	100
{r=1, p=8}	88.0	92.6	95.7	95.0	96.0	96.0	95.3
{r=1, p=16}	91.3	95.3	97.0	97.3	97.3	**98.0**	**98.0**

4 COPD Detection Using the Proposed 3D GMRF-based Method

We exploited our descriptor $GMRF_{P,R}^{3D}$ to detect COPD in given patients. The clinical dataset employed in this comparison is a set of full-lung HRCT volumetric images composed of 32 subjects where 19 subjects are healthy and 13 subjects were diagnosed with COPD. We extract volumes of interest (VOIs) from the HRCT images of lungs (see Figure 5) and the same process of our method described previously was carried out. The descriptor $GMRF_{8,1}^{3D}$ correctly classified 90.62% of subjects in the clinical dataset demonstrating that the GMRF is an efficient approach for texture characterization.

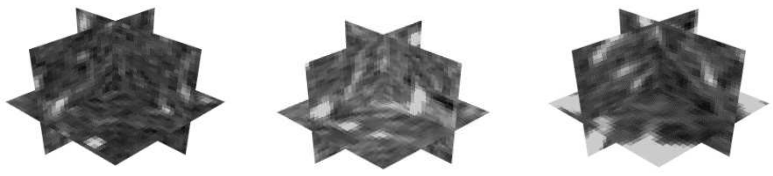

Fig. 5. VOIs sample taken from HRCT images of lungs in the clinical database.

To demonstrate the performance of our descriptor $GMRF_{P,R}^{3D}$ for detecting COPD in HRCT, we compared it against a 2D GMRF-based method called local parameter histogram (LPH) presented in [22]. To make this comparison fair, we used the same VOIs, parameters, and settings for both methods. We set $p = 8$ and $r = 1$ while the estimation window dimension was set to $w = 5$. Concerning histogram bins, we selected the number of histogram bins that scored the best accuracy. Regarding LPH, the method is applied to each 2D slice in the VOI and the best classification score among all these slices was selected.

Table 2 and Table 3 show, respectively, the classification accuracies and confusion matrices of the two compared descriptors which clearly demonstrate that our descriptor outperformed the 2D GMRF-based LPH method in detecting COPD in HRCT images. Despite the high computation time of our 3D GMRF-based method, the outcome of this comparison gives a cue that characterizing texture in 3D images provides more useful information compared with 2D images, which could contribute in the discriminatory power of extended 3D descriptors.

Table 2. Classification accuracies [%] for $\mathrm{GMRF}_{\mathrm{P,R}}^{\mathrm{3D}}$ and LPH.

Method	Accuracy [%]
$\mathrm{GMRF}_{8,1}^{\mathrm{3D}}$	90.62
LPH	75.00

Table 3. Confusion matrix for $\mathrm{GMRF}_{\mathrm{P,R}}^{\mathrm{3D}}$ and LPH.

$\mathrm{GMRF}_{8,1}^{\mathrm{3D}}$			LPH		
	Normal	Abnormal		Normal	Abnormal
Normal	17	2	Normal	11	8
Abnormal	1	12	Abnormal	0	13

5 Conclusion and Future Work

This paper proposes an extension of a 2D GMRF method to characterize textures in volumetric images. The method proposed here demonstrates excellent performance, achieving high classification accuracies when classifying a dataset of volumetric texture images. The discriminatory power of the descriptor is exploited to detect COPD using a clinical dataset. Our method shows a higher performance in comparison with the 2D GMRF-based method, using the same settings and criteria for the both methods.

An extension of this method to a rotationally invariant descriptor is our future plan to increase the discriminatory power in random rotated volumetric textures. In addition

to this, developing this method for segmentation purpose and reducing the feature dimension and time computation are also considered in our future work.

Acknowledgement: The CT data used in this work were acquired as a part of a study into the application of imaging to the characterization of the phenotypes of COPD. The written informed consent was given and signed by all subjects. The study was approved by the Southampton and South West Hampshire local research ethics committee (LREC number: 09/H0502/91) and the University Hospital Southampton Foundation Trust Research and Development Department. The study was conducted in the Southampton NIHR Respiratory Biomedical Research Unit. The research in this paper is funded by Technical and Vocational Training Corporation (TVTC) in Saudi Arabia.

References

1. Murray, Christopher J.L., Lopez, A.D.: Alternative projections of mortality and disability by cause 1990–2020. Global Burden of Disease Study. The Lancet, vol. 349.9064, pp. 1498–1504 (1997)
2. Decramer, M., Janssens, W., Miravitlles, M.: Chronic obstructive pulmonary disease. The Lancet, vol. 379, issue 823, pp. 1341–1351 (2012)
3. Vogelmeier, C., Criner, G., et al.: A global strategy for the diagnosis, management, and prevention of chronic obstructive lung disease report. GOLD Executive Summary. American Journal of Respiratory and Critical Care Medicine, vol.195, issue 5, pp. 557–582 (2017)
4. Sorensen, Lauge, Saher B., Shaker, De Bruijne, M.: Quantitative analysis of pulmonary emphysema using local binary patterns. IEEE Transactions on Medical Imaging, vol. 29, issue 2, pp. 559–569 (2010)
5. Müller, Nestor L., et al.: Density mask: an objective method to quantitate emphysema using computed tomography. Chest, vol. 94, issue 4, pp. 782–787 (1988)
6. Ojala, T., Pietikainen, M., Maenpaa, T.: Multiresolution gray-scale and rotation invariant texture classification with local binary patterns. IEEE Transactions on Pattern Analysis and Machine Intelligence, vol. 24, issue 7, pp. 971–987 (2002)
7. Pena, Isabel Pino, et al.: Automatic Emphysema Detection using Weakly Labeled HRCT Lung Images, arXiv preprint arXiv:1706.02051 (2017)
8. Heimann, T., Meinzer, H-P.: Statistical shape models for 3D medical image segmentation: a review. Medical Image Analysis, vol. 13, issue 4, pp. 543–563 (2009)
9. Guo, Zhenhua, et al.: Texture classification by texton: Statistical versus binary. PloS ONE, vol. 9, issue 2, e88073 (2014)
10. Xianghua, X., Mirmehdi, M.: A galaxy of texture features. Handbook of texture analysis, pp. 375–406 (2008)
11. Mao, J., Jain, A.K.: Texture classification and segmentation using multiresolution simultaneous autoregressive models. Pattern Recognition, vol. 25, issue 2, pp. 173–188 (1992)
12. Park, Yang Shin, et al.: Texture-based quantification of pulmonary emphysema on high-resolution computed tomography: comparison with density-based quantification and correlation with pulmonary function test. Investigative Radiology, vol. 43, issue 6, pp. 395–402 (2008)
13. Gao, Xiaohong, et al.: Texture-based 3D image retrieval for medical applications. IADIS Int. Conf. e-Health, (2010)

14. Citraro, Leonardo, et al.: Extended three-dimensional rotation invariant local binary patterns. Image and Vision Computing 62, 8-18, (2017)
15. Jain, Anil K., and Farshid Farrokhnia.: Unsupervised texture segmentation using Gabor filters. Pattern recognition 24.12 ,1167-1186 (1991).
16. Toriwaki, Junichiro, and Hiroyuki Yoshida.: Fundamentals of three-dimensional digital image processing. Springer Science & Business Media, (2009)
17. Depeursinge, Adrien, et al.: Three-dimensional solid texture analysis in biomedical imaging: review and opportunities. Medical Image analysis, vol.18, issue 1, pp. 176–196 (2014)
18. Dharmagunawardhana, Chathurika, et al.: Rotation invariant texture descriptors based on Gaussian Markov random fields for classification. Pattern Recognition Letters, vol. 69, pp. 15–21 (2016).
19. Petrou, M., Sevilla, P.G.: Image processing: dealing with texture. 1st edition: Chichester, Wiley, (2006)
20. Genschel, U., William Q.M.: A comparison of maximum likelihood and median-rank regression for Weibull estimation. Quality Engineering, vol. 22, issue 4, pp. 236-255 (2010).
21. Zhao, G., Pietikainen, M.: Dynamic texture recognition using local binary patterns with an application to facial expressions. IEEE Transactions on Pattern Analysis and Machine Intelligence, vol. 29, issue 6, pp. 915–928 (2007)
22. Dharmagunawardhana, Chathurika, et al.: Gaussian Markov random field based improved texture descriptor for image segmentation. Image and Vision Computing, vol. 32, issue 11, pp. 884–895 (2014)
23. Liu, X., DeLiang W.: Texture classification using spectral histograms. IEEE Transactions on Image Processing, vol. 12, issue 6, pp. 661–670 (2003)
24. OM, ANDERS BJ ORKSTR.: Ridge regression and inverse problems. Stockholm University, Department of Mathematics. (2001)
25. Friedman, J., Hastie, T., Tibshirani, R. The elements of statistical learning. 1st edition. New York: Springer series in statistics. (2001)
26. Paulhac, L., Makris, P., Ramel, Y-Y.: A Solid Texture Database for Segmentation and Classification Experiments. VISAPP vol. 2, (2009)
27. Xu, Ye, et al.: MDCT-based 3-D texture classification of emphysema and early smoking related lung pathologies. IEEE Transactions on Medical Imaging, vol. 25, issue 4, pp. 464–475 (2006)
28. Yao, Jianhua, et al.: Computer-aided diagnosis of pulmonary infections using texture analysis and support vector machine classification. Academic Radiology, vol. 18, issue 3, pp. 306–314 (2011)
29. Sorensen, Lauge, et al.: Texture-based analysis of COPD: a data-driven approach. IEEE Transactions on Medical Imaging, vol. 31, issue 1, pp. 70–78 (2012)
30. Tuceryan, M., Jain,A.K.: Texture analysis. Handbook of pattern recognition and computer vision, pp. 235–276 (1993)
31. Manjunath, B.S., Rama, C.: Unsupervised texture segmentation using Markov's random field models. IEEE Transactions on Pattern Analysis and Machine Intelligence, vol. 13, issue 5, pp. 478–482 (1991)
32. Rellier, G. et al. Texture feature analysis using a Gauss-Markov model in hyperspectral image classification. IEEE Transactions on Geoscience and Remote Sensing, vol. 42, issue 7, pp. 1543–1551 (2004)
33. Zhao, Yindi, et al.: Classification of high spatial resolution imagery using improved Gaussian Markov random-field-based texture features. IEEE Transactions on Geoscience and Remote Sensing, vol. 45, issue 5, pp. 1458–1468 (2007)